

RESEARCH ARTICLE

# Damage assessment of Nepal heritage through ambient vibration analysis and visual inspection

Russo Salvatore<sup>1</sup>  | Spoldi Eleonora<sup>2</sup> 

<sup>1</sup>Department of Design and Planning in Complex Environment, IUAV University of Venice, Italy

<sup>2</sup>IUAV University of Venice, Italy

## Correspondence

Eleonora Spoldi, IUAV University of Venice, Dorsoduro 2206, 30123 Venice, Italy.  
Email: espoldi@iuav.it

## Summary

The aim of this paper is to identify, both through microtremor analysis and visual inspection, the collapse mechanisms of the Nepalese wood-masonry monuments damaged by the 2015 seismic event that struck Kathmandu and its valley. The research analyses two case studies as the “Radha Krishna” temple located in Teku, a district in Kathmandu, and the “Pancha Deval complex” in Pashupati area. More specifically, after a careful anamnesis based on visual inspection and hypotheses on the temple’s structural behaviour, global nondestructive testing (microtremor) was carried out for qualitative characterization of the structural system. The visual damage survey allowed to identify the recurring collapse mechanisms in the two case studies with the identification of typical Nepali expected damage. The case of Radha Krishna temple denotes a Nepali collapse mechanism typical in the corner of temples made of timber masonry, in which the mechanical contribution of the timber is manifested through columns and windows. The ambient vibration analysis carried out by tromograph device and microtremor evaluation allowed to dynamically characterize the two bases by identifying the peak frequencies both for Radha Krishna and for Pancha Deval complex. With the same device, the two historic constructions have been also studied in evaluating local modes and frequency. In the Pancha Deval complex, a relationship between damage, frequencies, and the amplification of the base was observed. In detail, the five buildings have similar damage and similar first frequencies (2.72–2.9 Hz). The most damaged sides are those with the frequencies close to the base (2.05–2.38 Hz).

## KEYWORDS

ambient vibrations, damage assessment, Gorkha earthquake, microtremor, Nepal temple, tromograph

## 1 | INTRODUCTION AND METHODOLOGY

Nepal is located within the Himalayan mountain range, and it is the result of the subduction of the Indian plate under the Eurasian plate, initiated about 40–55 million years ago<sup>1</sup>. Record of past earthquakes show that Nepal felt two major earthquakes in the last 100 years. The 1934 Nepal–Bihar earthquake (M8) destroyed more than 80,000 buildings and claimed 8,500 lives<sup>2</sup>. The 2015 Gorkha earthquake (M7.8) destroyed half million homes, causing more than 8,790 deaths and 22,300 injuries<sup>3</sup>.

The evaluation of seismic damage in Nepal—according to the survey report by the Department of Archaeology—shows that 745 monuments in and around the Kathmandu Valley were damaged by the earthquake. The reports note that 133 monuments were in a totally collapsed state, 97 were partially collapsed, and 515 suffered partial damage. In Kathmandu Valley, 447 monuments were affected by the earthquake, out of which, 83 totally collapsed to the base<sup>4</sup>. Post seismic surveys of past earthquakes have shown the potential damage that unreinforced masonry structures (particularly pagoda temples) may suffer in a future earthquake. Most of Nepalese temples are considered non-engineered constructions that follow very simple rules and construction detailing in respect to seismic resistance requirements<sup>5</sup>.

There are some studies on the dynamic performance<sup>1,6</sup>, structural vulnerability<sup>7</sup>, and damage assessment<sup>8-10</sup> concerning the Nepalese Pagoda temples, but no studies on the Sikharas-style temple are present in scientific literature. Monumental structures and historic buildings are among the most vulnerable architectural typologies that can be affected by an earthquake<sup>11,12</sup>, and the dynamic performance of Nepalese Sikharas temple should be investigated<sup>13-15</sup>.

The evaluation of seismic damage, when supported by diagnostic tests, is a necessary tool to acquire the characteristics of a building, to identify its weaknesses, and to understand what are the best solutions to be implemented<sup>16-18</sup>. The knowledge of a building is essential to define the necessary action and intervention to improve the seismic capacity of the building<sup>19-21</sup>. For this reason, the diagnostic, especially non-destructive tests<sup>22-24</sup>, plays a fundamental role<sup>25,26</sup>.

The experimental investigation was carried out on two Nepali temples damaged by the 2015 Gorkha earthquake known as Radha Krishna temple (Teku) and Pancha Deval complex (Pashupati area). These temples are part of the heritage protected by UNESCO.

The damage assessment has been implemented through a very detailed visual investigation and using a digital portable tromometre for the dynamic investigation of the temples<sup>27,28</sup>.

## 2 | DESCRIPTION OF THE INVESTIGATED MONUMENTS

The two temples are Hindu monuments located in Kathmandu that are heavily damaged by the 2015 Gorkha earthquake. Both are UNESCO heritage sites and require structural rehabilitation interventions.

The Pancha Deval complex (Figure 1) is located in the Pashupati area, along the Bagmati River. It is currently used as a refuge for elderly people in financial difficulties. The complex was built in the 19th century, and it is composed of five buildings placed on an impressive base (Figure 1). The base has a square plan, 28 m per side, consisting of four decreasing upwards.

The five buildings have the same structural typology, identical architectural composition, and dimension. The only exception concerns the dimension of the central building, this building is 15 m long and 15 m tall. The other buildings are 13 m high, and they have a square plan, and they are composed by two floors (Figure 1a), only the first one is accessible (Figure 1b). The structure is masonry (brick-mud masonry), wooden floor, and the impressive roof is made of reinforced timber masonry (Figure 1c).

The Radha Krishna temple is a Sikharas-style temple located in Teku, a small district south of Kathmandu. It was built in the 19th century, and it is made of masonry, wood, and stone. The building is located on a masonry base (four steps), and it is 14 m tall (with base, Figure 2a). It has a square plan with central cell (Figure 2b). At the top of the base, there are 12 wooden columns near the masonry core<sup>29</sup>. The masonry on the ground floor is reinforced with wooden columns in the corners (Figure 2b,c) and an architrave system, also in timber, inside the cell (Figure 2d). The roofing system is given by an imposing masonry structure also reinforced with beams inside.

## 3 | DAMAGE ASSESSMENT THROUGH VISUAL INSPECTION

The buildings under study were severely damaged by the 2015 Gorkha earthquake, which hit Nepal with a magnitude of 7.8. After having identified the construction phases, it was decided to proceed to survey cracks and collapses to understand the actual damage level, observing the entire structure globally and locally. Both temples show a high structural damage that compromises their stability and safety.

The Radha Krishna temple has an externally undamaged roof; the masonry on the ground floor has completely lost its static capacity due to the complete expulsion of the corners. The building has not collapsed thanks to the timber colonnade. The colonnade has responded positively to the horizontal stress of the earthquake despite eight columns appear cracked and four columns need replacement (Figure 3a,b). The timber windows support the non-load-bearing

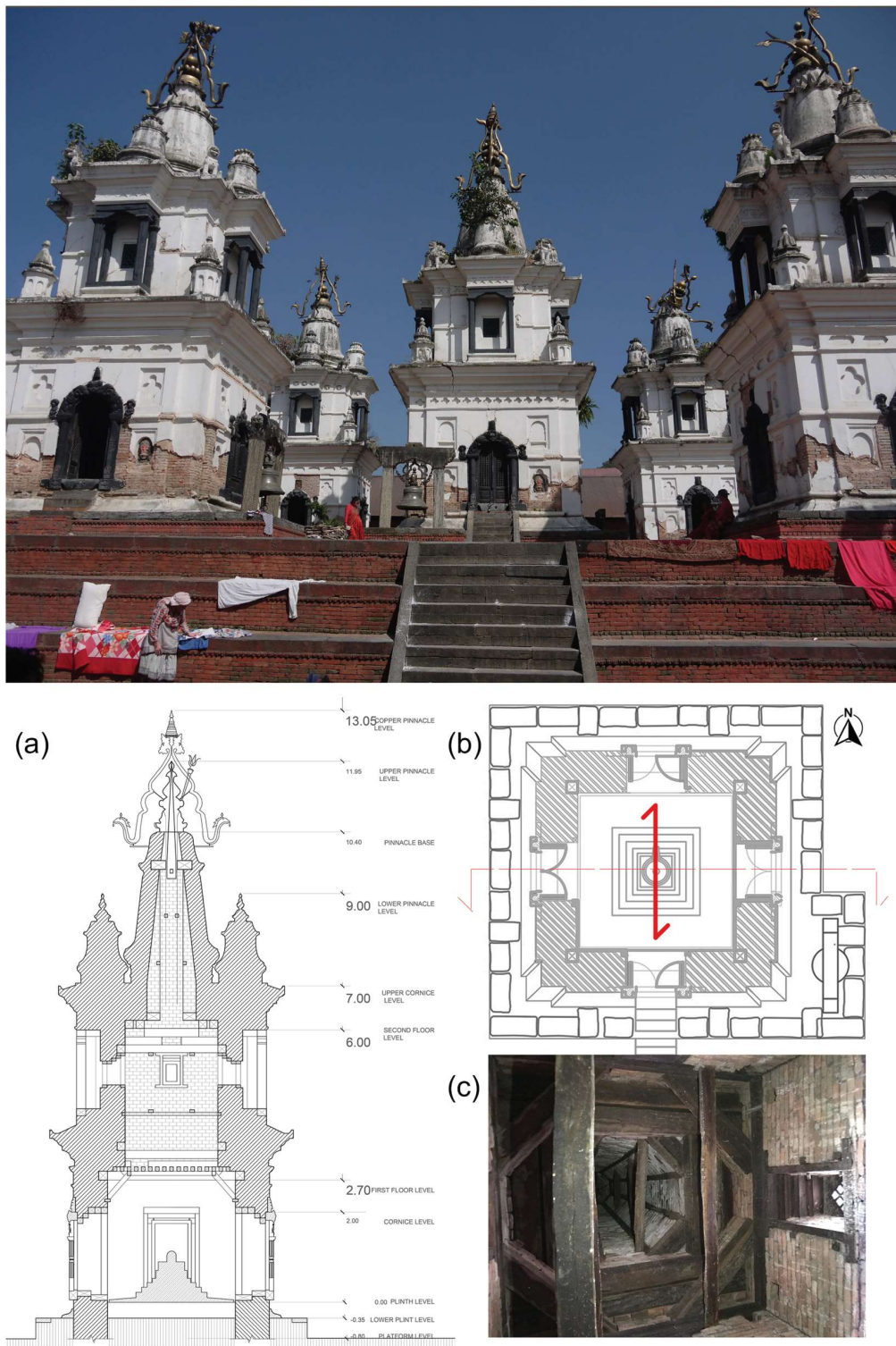


**FIGURE 1** Pancha Deval complex, (a) section, (b) ground floor, and (c) roof detail

wall. The windows are high as the ground floor, and they have played a fundamental role in the dissipation of energy induced by the earthquake. Currently, they present an out-of-plane mechanism but are still able to support the completely cracked masonry behind them (Figure 3c). The masonry of the ground floor is completely collapsed in the four corners (Figure 3d), and it is possible, observing the timber reinforcement. This reinforcement appears damaged or



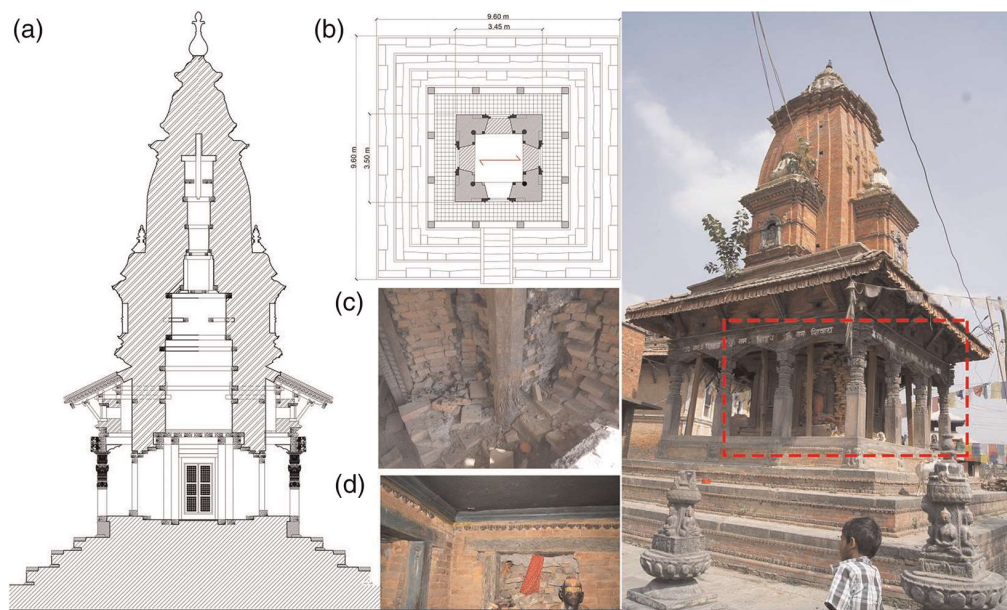


**FIGURE 2** Radha Krishna Temple, (a) cross section, (b) ground floor, (c) North–West corner, (d) inside view

without support. We can assume that the masonry has completely lost its function and the structure is supported by the timber elements (colonnade, architraves, and masonry interior columns).

The visible mud mortar joints are thick 1.5–2 cm, and the bricks have different dimensions, and they are not positioned in a regular way (Figure 3e). Punctual consolidation interventions without an overall and unitary strategy are present.

Observing the masonry of the ground floor, from the inside, it is possible to see on each side timber architrave systems inserted in the walls in correspondence with the external timber windows (Figure 3f). Also these timber reinforcements helped to dissipate the horizontal dynamic action. The architraves that make up these systems are inflected, and the wall beneath them is cracked.

Horizontal reinforcing timber elements were observed between the architraved systems and the external timber openings (Figure 3g).

The presence of vegetation is also an indication of the maintenance absence (Figure 3h).

The Pancha Deval complex presents in all buildings the different levels of damage. We observed a variation of the wall section between the ground floor and the upper floor. Specifically, the masonry on the upper floor has a larger section than the ground floor. The load generated by the masonry on the first floor is supported by the wooden floor reinforced by struts (inclined wooden elements) placed under it, which are discharge into the masonry on the ground floor.

Several cracks were observed at the base of the struts, in all temples. Many elements that make up the reinforcement of the roofs are deteriorated or absent. Other recurrent damage mechanisms observed in different buildings are cracks extended to the entire ground floor (Figure 4a). Radial cracks observable around the stone portal inserted in the wall that describe how the two materials of different stiffness have responded to the action of the earthquake. The stiffer stone has triggered breaking mechanisms in the masonry (Figure 4b). Diagonal cracks are visible near the wall corners with sliding along the horizontal direction of the bricks with possible ejection of the corners (Figure 4c). Important cracks in the cornices caused by the variation in geometry (Figure 4d) are present. Cracks are present (where vegetation is present) that allows water to enter, weakening already compromised structures (Figures 4e). Cracks “X” shape around the openings of the upper floors (Figure 4f) are visible. Wooden element deterioration inside the structure due to absence maintenance (Figure 4g) is visible.

## 4 | THE TROMOGRAPH DEVICE

For the dynamic modal characterization of the structures and the subsoil, we used the Tromino<sup>®</sup> device that optimizes the measurement of the microtremor in the frequency range between 0.1 and 200 Hz. The Tromino has a simple

**FIGURE 3** Global damage survey of Radha Krishna Temple



configuration; it is lightweight and compact, and it is easy to use everywhere. The small size ( $10 \times 14 \times 8$  cm), the lightness (1.1 kg), the batteries that allow the use without external cables, and the high resolution of the digital electronics parts make this instrument transportable<sup>30</sup>.

The device is equipped with three high-resolution electrodynamic velocimetric channels for the acquisition of the environmental seismic microtremor up to approximately  $\pm 1.5$  mm/s. The tromograph has also three velocimetric channels for recording strong vibrations up to  $\pm 5$  cm/s and three accelerometric channels. The sensors are located in three directions (terna x, y, and z) and transmit the signal to a digital acquisition system. The data recorded via tromograph



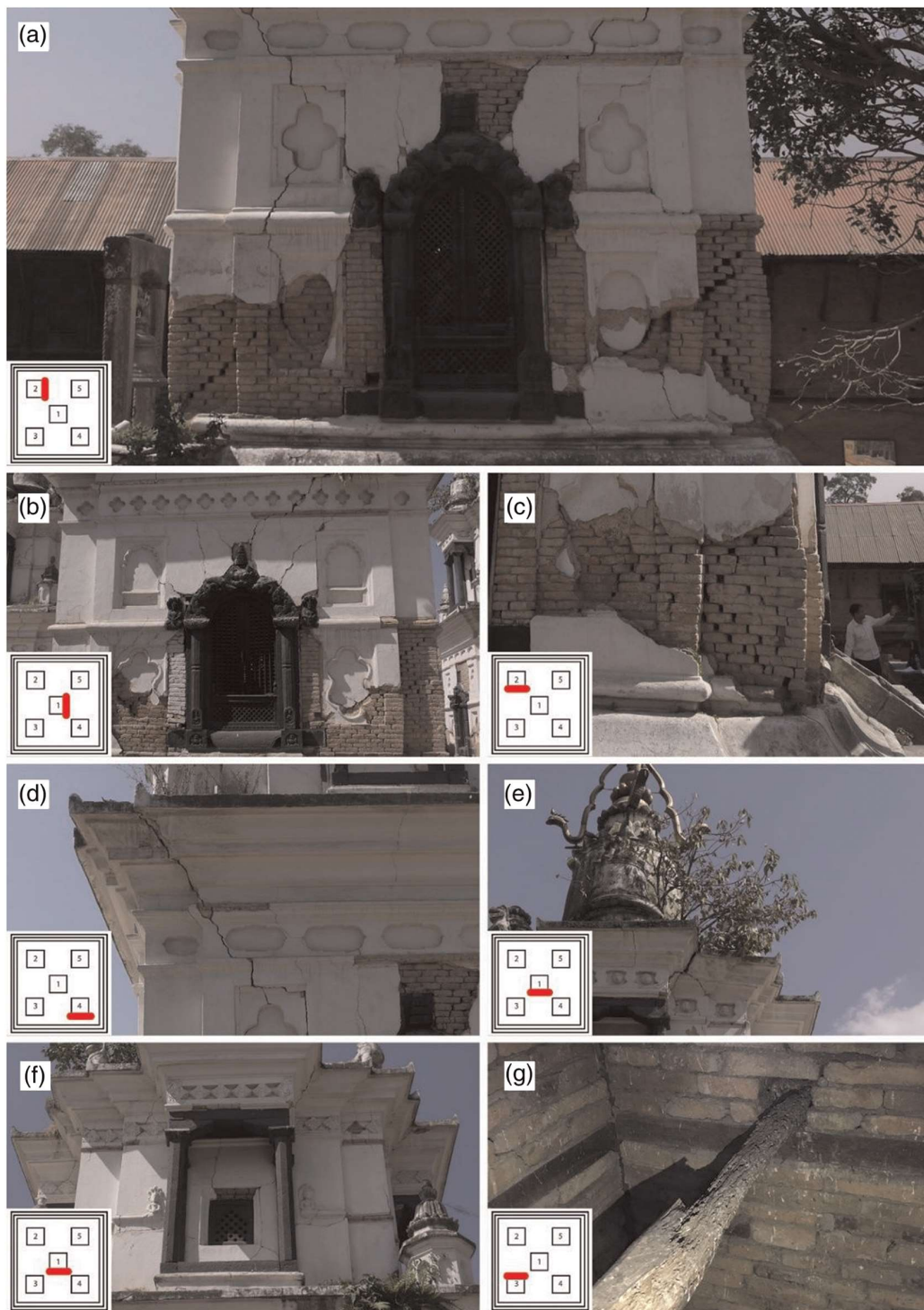


**FIGURE 4** Global damage survey of Pancha Deval Complex

are loaded into a specific software (Grilla<sup>®</sup>), which potentially performs frequency, modal shape, and damping coefficient.

An important part of the damage related to the effects of earthquakes in building is associated with the amplification of seismic waves caused by the site effect<sup>31</sup>. The performance frequency spectral ratio or horizontal to vertical spectra ratio is one of the most common approaches to determine that effect. This approach proposed first in

Mucciarelli and Gallipoli<sup>32</sup> and then by Nogoshi and Igarashi<sup>33</sup> is based on the initial studies of Kanai and Tanaka<sup>34</sup>. The test, born in Japan in 1970, is performed with a three-component seismometer. The tromograph software related to the Tromino allows to determine the site effect and use the well-known fast Fourier transform to obtain related spectra<sup>35</sup>. The fast Fourier transform is indicated through the following:

$$h(t) = \int_{-\infty}^{\infty} H(f) \exp(i2\pi ft) df = F[H(f)], \quad (1)$$

with  $h(t)$ : ( $t$ ) as variable function,  $F$  as Fourier transform, and  $H(f)$

$$H(f) = \int_{-\infty}^{\infty} h(t') \exp(-i2\pi ft') dt'. \quad (2)$$

It is to be noted that the functions  $h(t)$  and  $H(f)$  form a pair of Fourier transforms. The two variables  $t$  and  $f$  can be any pair of variables that have dimensions whose product is equal to 1.

The Fourier transform is produced by Equation (3):

$$h(t) = \sum_{n=-\infty}^{\infty} c_n \exp(i2\pi n f_0 t), \quad (3)$$

where if we allow the period  $T$  of the Fourier series to tend to be infinities, the frequency  $f_0$  tends to be zero, and in this way, an integral form of the Fourier series is obtained, which can also be used with non-periodic functions.

Then we proceed by calculating the ratio between the horizontal spectral component  $H$  and the vertical spectral component  $V$ ,  $H/V$  analysis. The frequencies in which this curve shows maximums, are the resonant frequencies of the site below the measurement point. This technique is suitable for the study of the ground.

Generally, the environmental noise is divided into two categories: natural and anthropic. Very often, especially in urban areas, this subdivision corresponds to different frequencies<sup>36</sup>. At low frequencies, less than 1 Hz, the origin is essentially natural: marine waves, coast-tide interaction, wind, unstable meteorological conditions, and thunderstorms. At high frequencies, above 1 Hz, the origin is mainly linked to human activities (traffic and industrial machinery), besides the  $H/V$  technique allows to eliminate from the recordings the noise's effect to obtain a stable curve with own resonance frequencies of the ground<sup>34</sup>.

It is possible to use the Tromino<sup>®</sup> for the dynamic identification of buildings. In this case, it is necessary to use an analysis that can eliminate the site effects. Building could be first assimilated to complex oscillators that vibrate with maximum amplitude only in correspondence of specific natural frequency. This condition does not occur not only when the structure is excited, like an earthquake, but also in the presence of environmental tremors. The practice is to place on the building one or more tromograph and record the time series  $f(t)$  for a few minutes.

Then the available mathematical tools, such as the Fourier transform, allow us to break down the  $f(t)$  series into a sum of elementary harmonics of Equation (4):

$$\sum A_i \sin(\omega_i t + \varphi_i), \quad (4)$$

in which  $A_i$  is the amplitude of the  $i$ th harmonic,  $\omega_i$  is the pulsation of the  $i$ th harmonic, and  $\varphi_i$  is the phase of the  $i$ th harmonic<sup>36</sup>.

The technique used to eliminate the effect of the underground site in structure investigated is called standard spectral ratio (SSR) while the analysis conducted to identify the vibration modes of the structure is a ratio between homologous  $H_i/H_0$  components (vertical or horizontal), able to identify different modal shape and amplify the frequencies<sup>37</sup>.

The sampling frequency chosen for our buildings' and bases' recording is 128 Hz, with 16 min. The duration of the registration is linked to the robustness of the statistical data. For a proper spectral resolution, the window has to be at least 10 times the period. In our case, we expect minor periods of less 2 s (frequencies higher than 0.5 Hz), adopting windows of 20 s. For an adequate statistic, the average is between 30–40 windows with a duration of not less than 20 s. The recording time cannot be less than 600–900 seconds or 10–15 min.

## 5 | DAMAGE ASSESSMENT THROUGH TROMOGRAPH

In the Radha Krishna temple, the tests were performed to identify the base peak frequencies for all sides, in the middle of each step.

In the Pancha Deval complex, 12 points of the main base were investigated, three on each side. The device was positioned on the ground, on half base and on the highest level. It was also possible to record the structures, positioning the device in the window compartments on the first floor of each single front of the complex.

### 5.1 | Base characterization through H/V approach

In the Pancha Deval complex, the traces related to the base were analysed with a 10% smoothing. The curves have only one clearly visible peak. The result of a single measurement is presented below. This measurement was recorded on the ground floor of the base, on the East side (Figure 5).

The recorded peak is 2.42 Hz and the “amplitude spectra” graph presents a curvature of the up-down curve as “ogive,” typical shape of the resonances of the ground. This curvature is in correspondence of the H/V maximum. Under normal conditions the spectral components NS, EW, and Z (vertical) have similar amplitudes. At the resonance frequency of the ground, the H/V analysis presents a maximum linked to a local minimum of the vertical spectral component, which determines an ogive shape like those indicated in the spectra below (Figure 5, dotted line).

This ogive shape is indicative of stratigraphic resonances<sup>38</sup>. Another indication, linked to the presence of ground resonance, is the shape of H/V maximum. This pick is large and close at twice of the peak frequency, and this is a typical condition of ground resonance. This situation also occurred in all other measurements carried out on the base of the Pancha Deval. Table 1 compares the individual peak frequencies of each measurement with the mean peaks obtained in the H/V analysis; in red are under light, the low frequencies.

The four H/V analyses, conducted on the four sides of the base, have only one peak that we can consider as the resonant frequency of the ground; the graphs of these analyses are shown in the image below (Figure 6).

It can be observed from Figure 6 that, when the height of the base increases, the amplitude of the spectra increases, except for the East side.

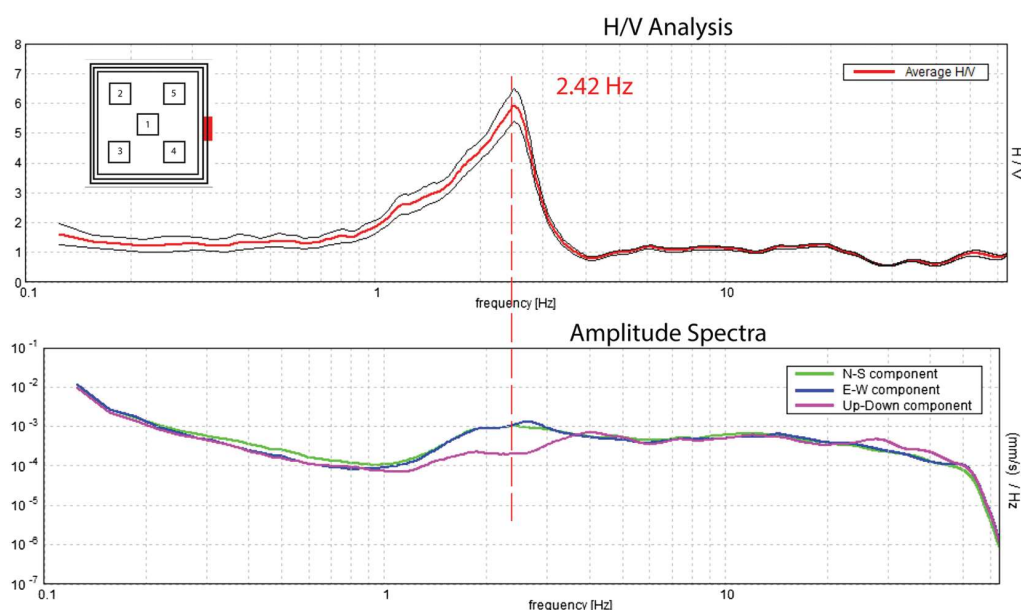


**FIGURE 5** H/V analysis (base ground floor, East front) and relative spectra



**TABLE 1** Peak base frequencies and mean H/V analysis of the Pancha Deval complex

Point	Orientation	Frequency (Hz)	Mean H/V (Hz)
Ground floor	South	2.19	2.2
Second step	South	2.22	2.2
Upper step	South	2.32	2.2
Ground floor	West	2.02	2.05
Second step	West	2.16	2.05
Upper step	West	2.21	2.05
Ground floor	North	2.29	2.30
Second step	North	2.37	2.30
Upper step	North	2.3	2.30
Ground floor	East	2.42	2.38
Second step	East	2.40	2.38
Upper step	East	2.41	2.38

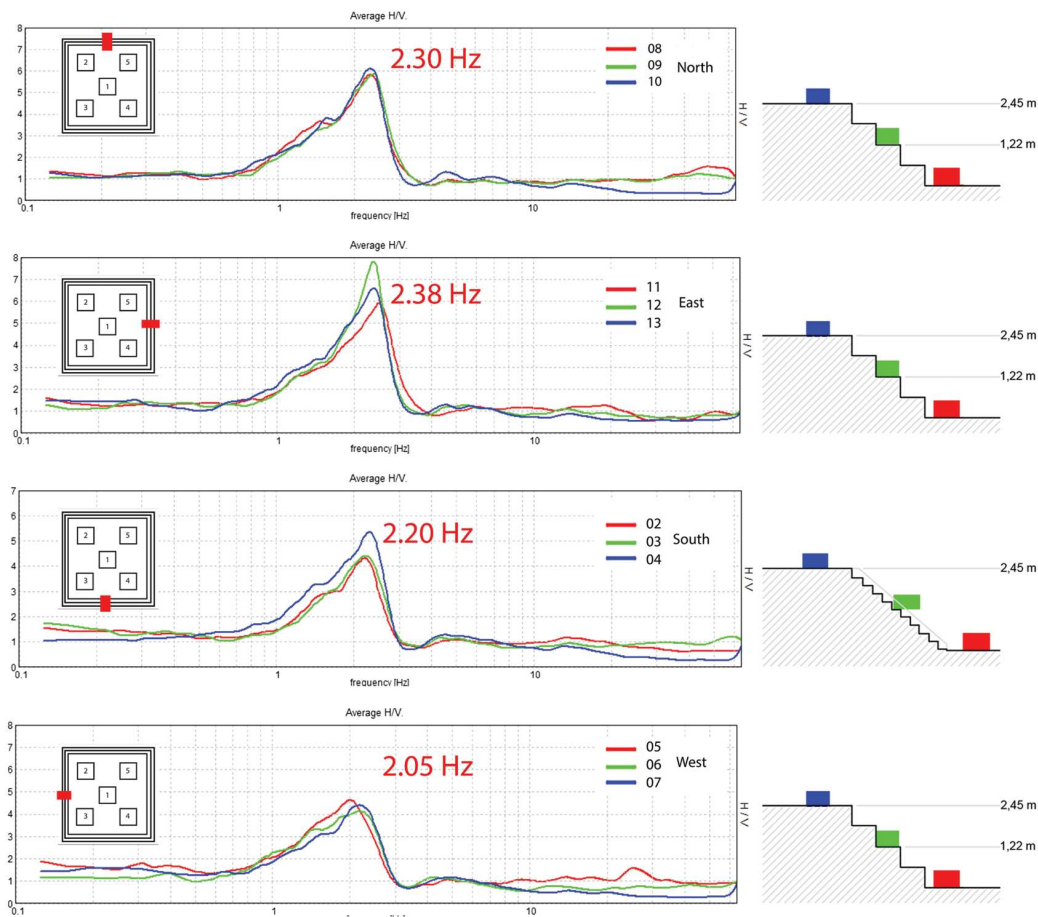


**FIGURE 6** H/V base curves of the Pancha Deval complex

The curves obtained from the recordings made on the base of the Radha Krishna temple are more difficult to read because they do not have an identifiable peak (Figure 7). In all the recording on the Radha Krishna base, the curves of H/V analysis have a maximum for frequencies lower than 1 Hz (Figure 7).

This result could be influenced by the presence of a river that flows 15 m from the building, which could be the main source of the low frequency of ambient microtremor.

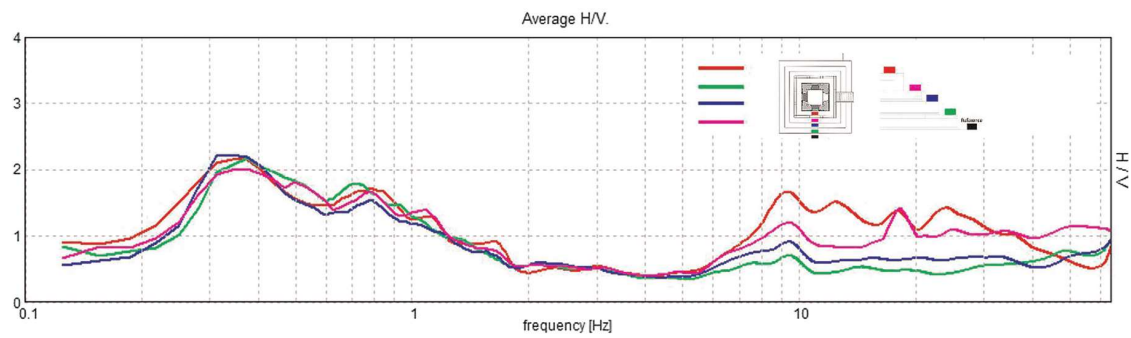


FIGURE 7 H/V base analysis, South-East front of the Radha Krishna temple

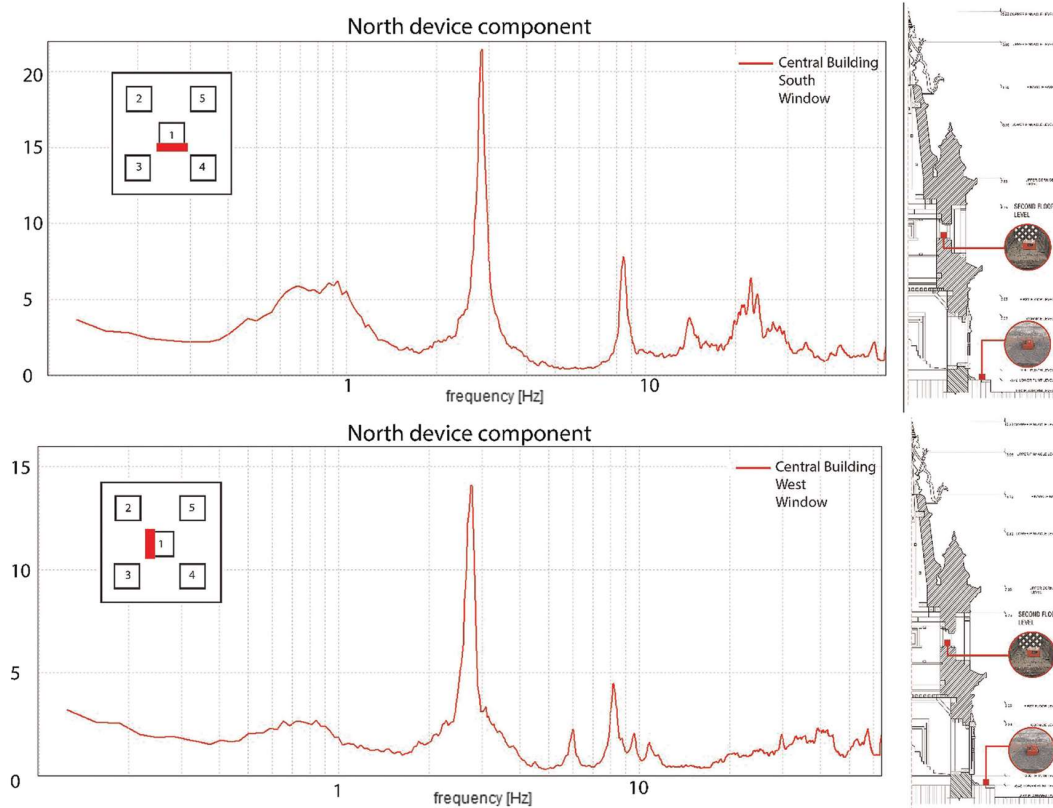


FIGURE 8 Ratio between homologous components, ground and first floor, South and West front, and central building

## 5.2 | Pancha Deval complex characterisation through SSR approach

Measurements were also carried out within the five buildings of the Pancha Deval complex to identify their fundamental frequencies. The instrument was positioned, for each side, at the base of the single building and in the respective first floor window.

In this case, the analysis (SSR) is a ratio analysis between homologous components ( $NS_i/NS_0$ ,  $EW_i/EW_0$ ) of single spectrum. The denominator measurement—reference measurement—is the measurement made on the base<sup>39,40</sup>.

In the test conducted in the southern fronts of the buildings, it is possible to identify three different natural frequencies. The amplitude of these frequencies decrease with the increase of Hz<sup>41</sup>. This behaviour was generally observed also in the North fronts. The following image shows this trend (Figure 8) and refers to the recording made in the window of the first floor of the South front of the central building.

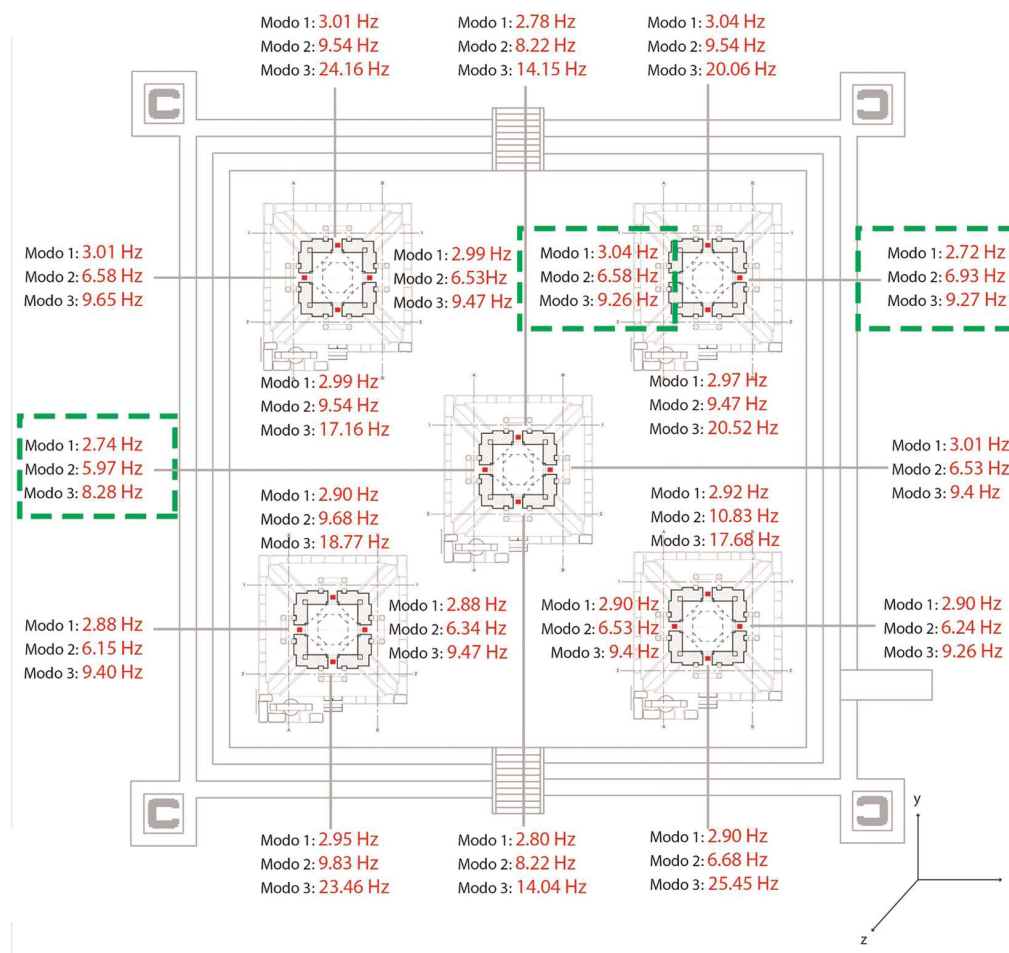


**FIGURE 9** Natural frequencies of Pancha Deval complex (window, first floor). Ratio between homologous instrumental North–South components

The East and West fronts present spectra with lower amplitude than the North and South fronts. The amplitude of these frequencies don't decrease with the increase of Hz. The amplitude of the second frequency is smaller than the third, and this could represent a torsion mechanism (Figure 8).

Figure 9 shows the SSR analysis of the first local vibration modes (North–South instrumental component). The distribution of frequencies is similar on the different fronts; in green, the lower frequencies are highlighted.

## 6 | DISCUSSION

The masonry of the Radha Krishna temple has been realized with low-quality materials. The mud mortar crumbles to the touch, and bricks of different sizes are positioned in an irregular way. A grey mortar is also visible, probably cement. This allows us to hypothesize that local rehabilitation interventions have been carried out following the damage reported by the structure but there hasn't a total rehabilitation intervention.

The corners have responded negatively to the action of the earthquake probably also due to the non-regular weaving of the masonry in the corner.

The timber elements of the structure have played a fundamental role in avoiding the complete collapse of the same. The ring beam system (placed at the base of the columns and at the top of the same), the columns, and the connection with the timber floor create a framework able to respond to the action of the earthquake by dissipating energy.

Four columns are completely cracked and need to be replaced; other five columns are cracked due to the earthquake and their stability is not compromised.



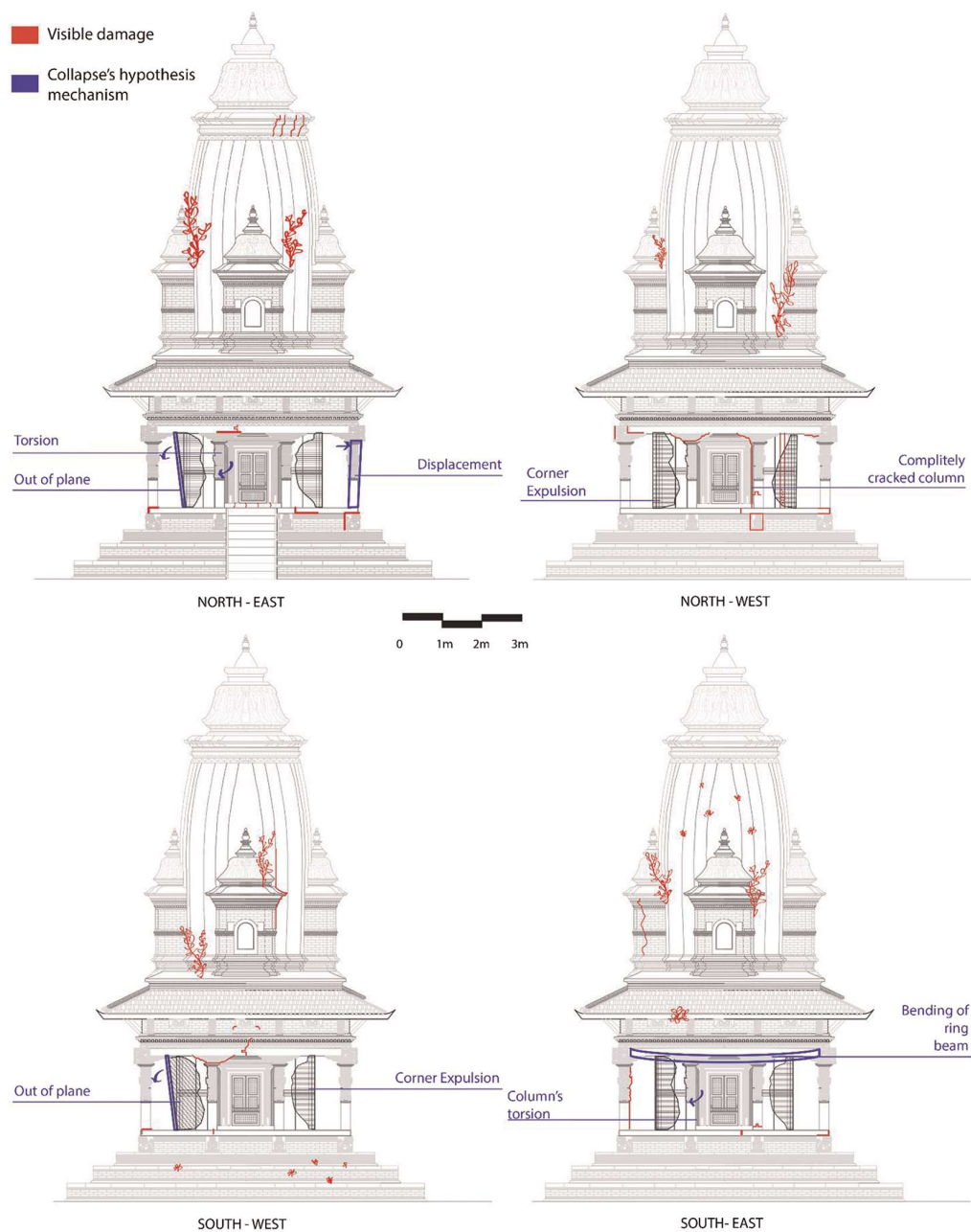


**FIGURE 10** Collapse's mechanism hypothesis, Radha Krishna Temple

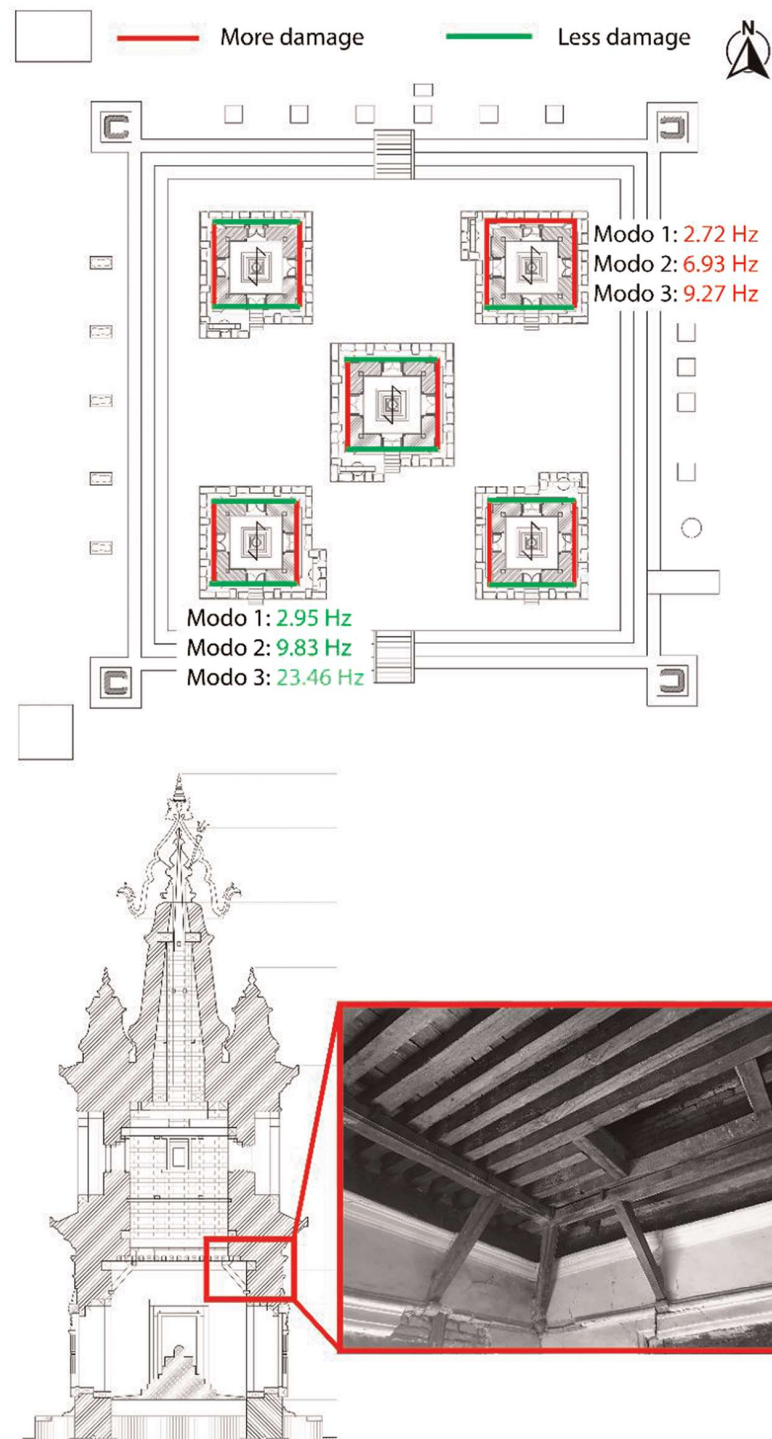
The full height wooden windows—directly connected to the wooden reinforcement inserted in the masonry—allowed to contain out of plan mechanism of the masonry placed behind them.

The surveys conducted on the base with the Tromino have curves without peaks in all the points investigated; this allows us to suppose that the base has a rigid block behaviour.

During the earthquake, the rigid base, characterized by small periods, transmits the action of the earthquake to the structure that is less rigid and made with low-quality masonry. The masonry responded to the energy transmitted by the rigid support plane with large displacements that triggered the high level of damage. Moreover, we can hypothesize that there is not a homogeneous dynamic behaviour between the base and the structure of the building with consequent major effect of the action of the earthquake.

Visual inspection confirms this hypothesis, and it has been observed that the four masonry corners on the ground floor have collapsed while the base didn't show any damage (Figure 10). The presence of only one horizontal diaphragm

**FIGURE 11** Collapse's mechanism, Pancha Deval complex. (a) Global hypothesis, (b) contribution due to timber elements



in a 14-m-high structure could have triggered torsion mechanisms with evident damage to the ground floor corners (Figure 10).

The lack of maintenance has allowed the vegetation to grow between the mortar joints. This phenomenon had weakened the structure and allowed the water to enter in the masonry.

The visual inspection conducted in the five buildings of the Pancha Deval complex helps us understand how the masonry's thickness changes near the horizontal diaphragm (Figure 11, red square). In detail, the first floor masonry is thicker than the ground floor. Therefore, the former has a bigger load than the latter and this load is transferred to the

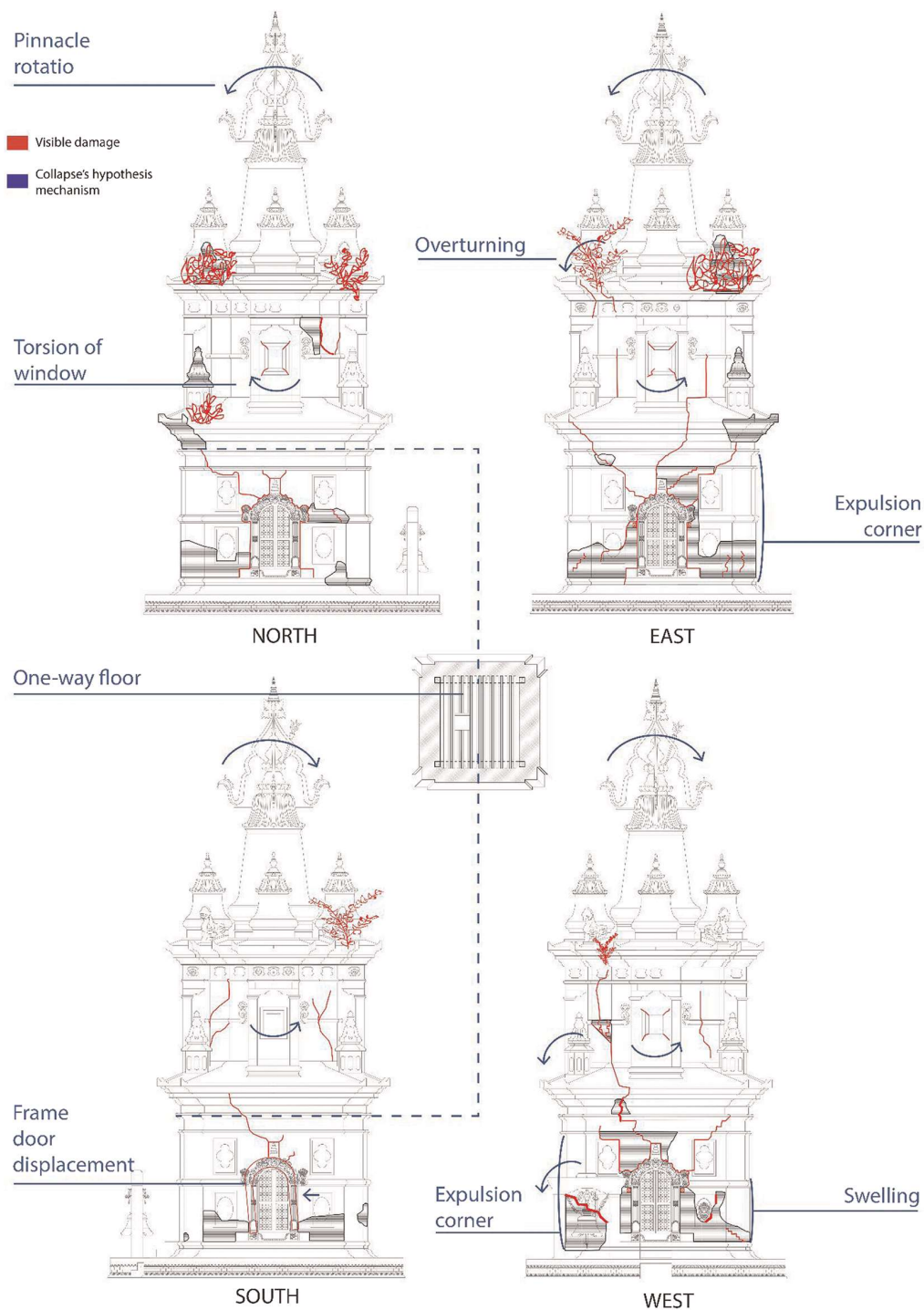


**FIGURE 12** Collapse's mechanism, Pancha Deval complex, North East temple

struts, which then transfer it to the ground floor. It has been found that near the base struts, the damage is considerable.

In particular, the North and South fronts, supporting the plane of the beams, are less damaged while the East and West front are more damaged (Figure 11).

The difference in damage between the North–South and East–West fronts is also visible from the outside. The sides not bound by the floor (East and West) have important diagonal cracks on the ground floor.



**TABLE 2** Local vibration mode, Pancha Deval complex

Mode		East			North			South			West		
		NSi/ Ns0 (Hz)	EWi/ EW0 (Hz)	Zi/ Z0 (Hz)	NSi/ Ns0 (Hz)	EWi/ EW0 (Hz)	Zi/ Z0 (Hz)	NSi/ Ns0 (Hz)	EWi/ EW0 (Hz)	Zi/ Z0 (Hz)	NSi/ Ns0 (Hz)	EWi/ EW0 (Hz)	Zi/ Z0 (Hz)
B1	M1	3.1	3.32	2.86	2.78	2.86	2.8	2.8	2.86	2.76	2.74	2.9	2.82
	M2	6.53	10.2	12.65	8.22	6.02	14.25	8.22	6.02	7.52	5.97	8.22	14.25
	M3	9.4	20.06	16.05	14.15	8.34	15.82	14.04	8.28	14.04	8.28	21.61	19.77
B2	M1	2.99	3.17	3.1	3.01	3.02	2.97	2.99	3.27	2.88	3.1	3.27	3.74
	M2	6.53	10.28	15.47	9.54	6.58	15.01	9.54	6.48	14.9	6.58	10.35	14.9
	M3	9.47	24.89	28.46	24.16	9.83	25.14	17.16	9.97	22.77	9.65	20.98	22.77
B3	M1	2.88	3.17	2.9	2.9	3.13	3.5	2.95	3.08	2.99	2.88	3.08	3.06
	M2	6.34	10.28	16.05	9.68	6.34	13.23	9.83	6.38	11.4	6.15	10.43	9.68
	M3	9.47	19.77	18.77	18.77	9.97	25.84	23.46	10.05	17.4	9.4	19.9	16.29
B4	M	2.9	3.04	3.06	2.92	3.01	2.82	2.9	3.06	2.7	2.9	3.49	16.29
	1												
	M	6.24	10.43	16.5	10.83	6.38	9.93	6.68	6.1	9.37	6.53	6.33	29.32
	2												
	M3	9.26	20.36	28.88	17.68	10.43	15.82	25.45	9.34	15.37	9.4	19.77	41.58
B5	M1	2.72	3.2	3.27	3.04	3.08	3.01	2.97	3.22	3.85	3.04	3.27	3.01
	M2	6.93	10.43	10.9	9.54	6.68	14.79	9.47	6.53	15.24	6.58	10.74	15.93
	ME	9.27	19.77	16.05	20.06	10.28	21.94	20.52	10.51	28.46	9.26	19.77	26.22

The framework of windows and stone's door have triggered radial and “X” cracks near the openings due to the difference in stiffness between the stone and the masonry (Figure 12). Other important cracks are visible near the vegetation and near the moulding.

The masonry pinnacles—placed in the four corners of the first level cornice—unload their weight on the corner, weakening the corner and triggering cracks at their base (Figure 12).

The H/V analysis conducted on the Pancha Deval complex base shows resonance frequency in the range 2.05–2.38 Hz. When the height of the base increases, the amplitude of the spectra and frequencies increases, except for the East side. Recalling the formula  $f = nVs/4H$ , where  $n$  indicates the order of the vibrating mode (fundamental, first higher etc.),  $H$  is the thickness between interface of the seismic bedrock and less rigid sedimentary cover, and  $Vs$  is the velocity of the cutting waves<sup>34</sup>, we would expect that as the denominator increases (the height  $H$ ) the frequency decreases, but it is not our case. This allows us to hypothesize that the base is not simply filled with soil but with stiffer materials, such as masonry.

Overall, the visual inspection has shown that in all the buildings of the Pancha Deval complex, the East and West fronts are more damaged than the North and South fronts. The measures of the environmental microtremor, conducted on the structures, confirm this overall difference. In fact, the SSR analyses show a variation in frequencies—so a variation in stiffness—between the different meters but show the same frequencies for homologous front of the different buildings.

Table 2 shows in green the frequencies related to the temple placed in the North–West corner of the base, which has higher frequencies, and it is visibly less damaged than the others. The frequencies (in red) of the building located in the North East corner of the base, which has lower frequencies, and it is visually the most damaged building.

Overall, it has been observed that the ratio between the components  $NS_i/NS_0$  and  $EW_i/EW_0$ , relative to the plane considered perpendicular to the height of the structure, has lower average frequencies. The curve of  $Z_i/Z_0$  analysis has higher frequencies but smaller amplitudes than the corresponding horizontal components.

Figure 13 compares the H/V analysis conducted on the West side of the base and the SSR analyses conducted on the West elevation of the central building. The H/V maximum of the base and SSR maximum of the building are in the same frequency range with different amplitudes.

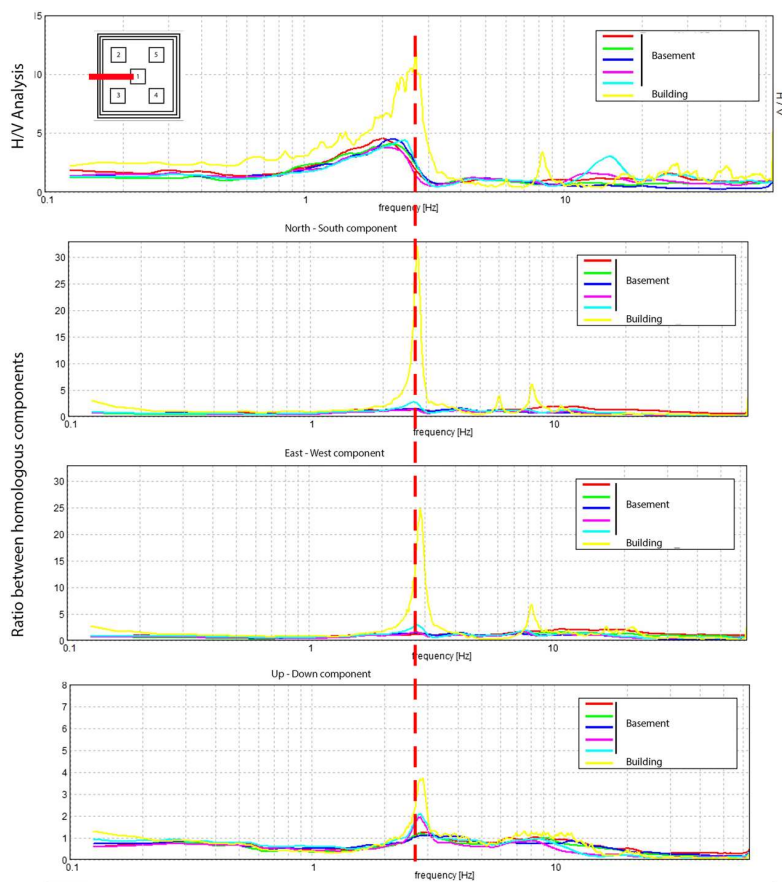


**FIGURE 13** H/V Analysis and ratio between homologous components, side West central Temple

The North–South and East–West curves have a first peak with amplitude greater than the 25 factor, while the up–down curve has an amplitude less than 4.

During the action of the earthquake, the similar dynamic behaviour between base and structure has triggered a phenomenon of amplification of the action with a significant effect on the structures, in particular in the East and West fronts of the buildings. The red line (Figure 12) ideally connects the different first natural frequency of the curves.

## 7 | CONCLUSION

The Radha Krishna temple has a high level of damage. The damage is mainly concentrated on the masonry of the ground floor, which has completely lost its structural validity and is about to collapse. The presence of important timber structural element—inside and outside the masonry—has prevented the complete collapse of the building. The corner expulsion denotes a Nepali collapse mechanism typical in corner made by timber masonry, in which the mechanical contribution of the timber is manifested through columns and windows. The analyses conducted with the tromograph on the base show how the ground has resonance frequencies at 0.35 Hz. The difference in stiffness between a very rigid ground and the mud masonry temple influenced the earthquake effects, and the results are visible on the ground floor.

Also, in the Pancha Deval complex, the presence of timber struts was instrumental. The timber elements have dissipated the earthquake by supporting the masonry. The structural damage in the complex is similar for all five buildings. Important diagonal cracks are visible in the masonry of the ground floor of the East and West fronts; these fronts aren't bounded by the timber floor. Other important cracks are visible at the base of the struts and at the point of contact between material with different stiffness (stone masonry). The lush vegetation shows a lack of maintenance of the entire complex.

The base has natural frequencies in the 2.5–2.42 Hz range. The West side has lower frequencies, and the east side has greater amplitudes in the H/V curve. This allows us to hypothesize that the base is stiff and partly filled with masonry. The spectral analyses conducted in the buildings show similar natural frequencies ranging between 2.72 and 3.74 Hz with lower frequencies (2.75–2.99 Hz) in the East fronts of the buildings. Similar frequencies between base and buildings allow us to hypothesize that the amplification of the earthquake due to the base is not negligible<sup>42</sup>. The Southern facades have higher overall frequencies for the different vibration modes, with respect to the East and West fronts, with possible torsional modes. Besides, the visual inspection and the survey of the structural damage have shown that the East and West fronts have a structural damage, greater than the other fronts.

The interaction between tromograph and visual inspection proves to be very useful for the Radha Krishna and Pancha Deval Temples. That is also a rapid and in-depth methodology of analysis with an evident high correspondence between higher frequency and higher level of damage.

## ACKNOWLEDGEMENTS

Thanks to the UNESCO office in Kathmandu for economic support in situ. We especially thank the student Giulia Capuzzo who in the mission carried out in Nepal (October–December 2017) has collaborated with us in completing the contract with UNESCO Nepal, aimed at the analysis of the damage and expected seismic behaviour of the two monumental structures object of the paper.

## ORCID

Russo Salvatore  <https://orcid.org/0000-0002-2627-2624>

Spoldi Eleonora  <https://orcid.org/0000-0002-1510-9549>

## REFERENCES

1. Bijaya, J., Wei-Xin, R., Zhou-Hong, Z., Prem, N.M., *Dynamic and seismic performance of old multi-tiered temples in Nepal*. *Engineering Structures*, 2003, 25, 1827–1839.
2. United Nations Office for the Coordination of Humanitarian Affairs (OCHA). Nepal: Preparing for an earthquake in the Kathmandu Valley, 2013. Available online: <http://www.unocha.org/story/nepal-preparing-earthquake-kathmandu-valley>.
3. Lizundia, B., Davidson, R.A., Hashash, Y.M.A., Olshansky, R. Overview of the. *Gorkha, Nepal, earthquake and the earthquake spectra special issue*. *Earthquake Spectra*. 2015;2017(33):S1–S20. <https://doi.org/10.1193/120817EQS252M>
4. Department of Archeology (DoA). *Preliminar list of affected monuments of Nepal by Gorkha Earthquake*, 2015, Kathmandu, Nepal
5. Shakya M, Varum H, Vicente R, Costa A. *Seismic sensitivity analysis of the common structural components of Nepalese Pagoda temples*. *Bull Earthquake Eng*. 1679–1703;2014(4):12–1703. <https://doi.org/10.1007/s10518-013-9569-6>
6. Wood, R.L., Mohamemmadi, M.E., Barbosa, A.R., Abdulrahman, L., Soti, R., Kawan, C.K., Shakya, M., Olsen, M.J. *Damage assessment and modelling of the five- tiered pagoda – style Nyatapola temple*. *Earthquake Spectra* 2017, 33– S377–S384
7. Shakya M, Varum H, Vicente R, Costa A. *Seismic vulnerability and loss assessment of the Nepalese Pagoda temples*. *Bull Earthquake Eng*. 2015;13(7):2197–2223. <https://doi.org/10.1007/s10518-014-9699-5>
8. Theophile, E., Ranjitkar, R.K. *Timber conservation problems of the Nepalese Pagoda temple*. In: Proc. ICOMOS International Wood Committee, 8th International Symposium, Kathmandu, 1992, 85–124.
9. Shrestha, S., Shrestha, B., Shakya, M., Maskey, P.N. *Damage assessment of cultural heritage after the 2015 Gorkha, Nepal, earthquake: a case study of Jagannath Temple*. *Earthquake Spectra* 2017, 33, S363–S376. <https://doi.org/10.1193/121616EQS241M>.
10. Joshi, V.M., Kaushik, H.B., *Historic earthquake-resilient structures in Nepal, other Himalayan regions, and their seismic restoration*. *Earthquake Spectra* 2017, 33, S299–S319
11. Lagomarsino, S. and Podestà, S. *Damage and vulnerability assessment of the churches after the 2002 Molise, Italy earthquake*, *Earthquake Spectra*, 2002, 20, 271–283.
12. Italian Guidelines (2010) *Guidelines for evaluation and mitigation of seismic risk to cultural heritage with reference to technical standard for construction*, Ministry for Cultural Heritage and Activities, Dept. of Civil Protection Agency; Adopted with Prime Minister Directive, 12 October, 2007, G.U. n. 24 of 29/01/2008, Gangemi Editor, Rome, Italy (in Italian).
13. Korn, W. *The traditional architecture of the Kathmandu Valley*,. Bibliotheca Himalaya. *Kathmandu*. 1976.
14. Bonaparte C, Sestini V. *Il mandala nel progetto: storie e tradizioni costruttive in Nepal*. *Bioarchitettura*. 2014;84:34–39.
15. Dangol, P. *Elements of the Nepalese temple architecture*. *Adroit*. New: Delhi; 2011.
16. Russo S. *On the monitoring of historic anime Sante church damaged by earthquake in L'Aquila*. *Structural Control and Health Monitoring*. 2012;20:1226–1239.
17. Ubertini, F., Comanducci, G. and Cavalagli, N. (2017) 'Earthquake-induced damage detection in a monumental masonry bell-tower using long-term dynamic monitoring data', *Bulletin of Earthquake Engineering*, September 2017, doi: <https://doi.org/10.1007/s10518-017-0222-7>.



18. Syrmakezis CA. *Seismic protection of historical structures and monuments*. *Struct. Control Health Monit.* 2006;13:958-979. <https://doi.org/10.1002/stc.89>
19. El-Borgi S, Smaoui H, Casciati F, Jerbi K, Kanoun F. Seismic evaluation and innovative retrofit of a historical building in Tunisia. *Structural Control Health Monitoring*. 2005;12:179-195.
20. Celebi, M. *Seismic instrumentation of buildings*, U.S. Dept, of the Interior, U.S. Geological Survey, Open-File Report 2000,157, 37.
21. Sepe V, Speranza E, Viskovic A. *A method for large-scale vulnerability assessment of historic towers*. *Struct. Control Health Monit.* 2008;15:389-415. <https://doi.org/10.1002/stc.243>
22. Brando G., Rapone D., Spacone E., O'Banion M. S., Olsen M. J., Barbosa A. R., Faggella M., Gigliotti R., Liberatore D., Russo S., Sorrentino L., Bose S., Stravidis A. *Damage reconnaissance of unreinforced masonry bearing wall buildings after the 2015 Gorkha, Nepal, earthquake*. *Earthquake spectra*, 2017, vol. 33, p. 243-273, ISSN: 8755-2930, doi: 10.1193/010817EQS009M
23. Russo, S. *Integrated assessment of monumental structures through ambient vibration an ND test: the case of Rialto Bridge*. *Journal of cultural heritage*, 2016, 19, 402-414, ISSN: 1296-2074, DOI: 0.1016/j.culher.2016.01.008
24. Bassoli E, Vincenzi L, D'Altri AM, de Miranda S, Forghieri M, Castellazzi G. Ambient vibration-based finite element model updating of an earthquake-damaged masonry tower. *Struct Control Health Monit.* 2018;25:1-15. <https://doi.org/10.1002/stc.2150>
25. Gentile C, Saisi A. *Ambient vibration testing of historic masonry towers for structural identification and damage assessment*. *Construction and Building Materials*. 2007;21:1311-1321.
26. Binda L, Saisi A. *Research on historic structures in seismic areas in Italy*. *Progress in Structural Engineering and Materials*. 2005;7(2):71-85.
27. Vicente, R.S., Parodi, S., Lagomarsino, S., Varum, H. and Mendes da Silva JAR. *Seismic vulnerability and risk assessment: case study of the historic city centre of Coimbra, Portugal*, *Bull. Earthq. Eng.*, Vol. 9, No. 4, pp.1067-1096.
28. Castellaro S, Perricone L, Bartolomei M, Isani S. *Dynamic characterization of the Eiffel tower*. *Engineering Structures*. 2016;126:628-640.
29. Pau, A. and Vestroni, F. *Vibration assessment and structural monitoring of the Basilica of Maxentius in Rome*, *Mechanical Systems and Signal Processing*, 2013, Vol. 41, Nos. 1-2, pp.454-466.
30. Strobbia, C., Cassiani, G. *Refraction microtremors: data analysis and diagnostic of key hypotheses*. *Geophus*, 2011,76, MA11-MA20
31. Korn, W. *The traditional Newar architecture: the Sikharas*. Ratna Pustak Bhandar, 2014, Kathmandu
32. Mucciarelli M, Gallipoli MR. *A critical review of 10 years of microtremor HVRS technique*. *Boll. Geofis. Teorica*. 2001;42:255-266.
33. Nakamura Y. *A method for dynamic characteristics estimates of subsurface using microtremor on the round surface*. *QR of RTRI*. 1989;30:25-33.
34. Nogoshi M, Igarashi T. *On the propagation characteristics of microtremors*. *Seism. Soc. Japan*. 1970;23:264-280.
35. Chopra, A. K., *Dynamics of structures: theory and applications to earthquake engineering*, Pearson; 2015
36. SESAME Project, *Guidelines for the implementation of the H/V spectral ratio technique on ambient vibrations. Measurements, processing and interpretation, WP12, deliverable no. D23.12*, [http://sesame-jp5.obs.uhf-grenoble.fr/Papers/H/V\\_User\\_Guidelines.pdf](http://sesame-jp5.obs.uhf-grenoble.fr/Papers/H/V_User_Guidelines.pdf)
37. Albarello D., Castellaro S. *Tecniche sismiche passive: indagini a stazione singola*. Supplemento alla rivista ingegneria sismica, 2011, XXVIII, 2, 32-50.
38. Snieder, R., Safak, E. *Extracting the building response using seismic interferometry: theory and application to the Millikan Library in Pasadena, California*, *Bull. Seismol. Soc. Am.*, 2006, 96, 586-598
39. Castellaro, S., *Caratterizzazione dinamica del sottosuolo ai fini dell'ingegneria sismica*, <http://www.cias-italia.it/PDF/castellaro.caratterizzazione%20dinamica%20del%20sottosuolo%20ai%20fini%20dell'ingegneria%20sismica.pdf>
40. Gallipoli MR, Mucciarelli M, Castro RR, Monachesi G, Contri P. *Structure, soil-structure response and effects of damage based on observations of horizontal-to-vertical spectral ratios of microtremors*. *Soil Dynamics and Earthquake Engineering*. 2004;24:487-495.
41. Russo, S., Liberatore, D., Sorrentino, L., *Combined ND techniques for structural assessment: the case of Historic Nepali constructions after the Gorka earthquake*, *ICEM 2018. Brussels, July*. 2015;2018:1-5.
42. Castellaro, S., Raykova, R.B., Tsekov, M., *Resonance frequencies of soil and buildings-some measurements in Sofia and its Vicinity*, 3rd National congress on Physical Sciences, 29 Sep. - 2 Oct. 2016, Sofi

**How to cite this article:** Russo S, Spoldi E. Damage assessment of Nepal heritage through ambient vibration analysis and visual inspection. *Struct Control Health Monit.* 2020;e2493. <https://doi.org/10.1002/stc.2493>